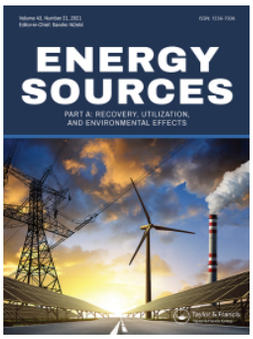

Taylor & Francis
Taylor & Francis Group

Energy Sources, Part A: Recovery, Utilization, and Environmental Effects

ISSN: 1556-7036 (Print) 1556-7230 (Online) Journal homepage: www.tandfonline.com/journals/ueso20

A computationally efficient jaya optimization for fuel cell maximum power tracking

Ramesh Gugulothu, Bhookya Nagu & Deepak Pullaguram

To cite this article: Ramesh Gugulothu, Bhookya Nagu & Deepak Pullaguram (2022) A computationally efficient jaya optimization for fuel cell maximum power tracking, Energy Sources, Part A: Recovery, Utilization, and Environmental Effects, 44:1, 1541-1565, DOI: 10.1080/15567036.2022.2055229

To link to this article: https://doi.org/10.1080/15567036.2022.2055229

ENERGY SOURCES, PART A: RECOVERY, UTILIZATION, AND ENVIRONMENTAL EFFECTS
2022, VOL. 44, NO. 1, 1541–1565
https://doi.org/10.1080/15567036.2022.2055229

Taylor & Francis
Taylor & Francis Group

A computationally efficient jaya optimization for fuel cell maximum power tracking

Ramesh Gugulothu, Bhookya Nagu, and Deepak Pullaguram

Department of Electrical Engineering, National Institute of Technology Warangal, Telangana, India

ABSTRACT

Fuel cells typically exhibit non-linear, convex P – I characteristics with a single peak power-point for a constant temperature, membrane water content (MWC), hydrogen gas, and oxygen partial pressure. In this paper, a Jaya algorithm-based maximum power point tracking (MPPT) is developed for fast and accurate peak power tracking of a proton exchange membrane fuel cell (PEMFC). Most of the conventional MPPT algorithms are prone to continual steady-state oscillations. Further, most meta-heuristic MPPT algorithms use a PID controller to track the peak power-point. The use of combined meta-heuristic and PID controller affects the efficiency of MPPT since it is strongly dependent on PID controller gains and meta-heuristic optimization parameters. In this paper, a Jaya algorithm-based MPPT tracking approach without a PID controller is developed to fulfill the MPP of a PEMFC. The Jaya algorithm-based MPPT solution ensures a global maximum peak power-point solution that is independent of solver parameters. The efficacy of the proposed Jaya MPPT is evaluated by performing various simulation studies under various operating conditions with different perturbations and compared against widely accepted particle swarm optimization (PSO), conventional perturb and observe (P&O)-based MPPT techniques. The proposed method can track a maximum power of 1411.02 W within two iterations as compared to method particle swarm optimization (PSO), conventional perturb and observe (P&O), which could track a maximum power of 1376.11 W and 1370.4 W, respectively. Thus, giving an additional increase in power efficiency 2.53% Jaya algorithm. Furthermore, the proposed approach delivered an improved output power efficiency of 11.28% compared to the fuel cell operation without MPPT. Further, the real-time feasibility of the proposed algorithm is also validated by developing a hardware prototype and performing various case studies to track MPPT under different operating conditions and perturbations.

ARTICLE HISTORY
Received 30 August 2021
Revised 28 February 2022
Accepted 10 March 2022

KEYWORDS
Fuel cells; jaya algorithm; maximum power point tracking (MPPT); meta-heuristic; optimization

Introduction

Global warming, gradual depletion of fossil fuels, and public awareness about carbon emissions have made researchers explore alternate solutions for energy production. The use of renewable energy resources (RESs), fuel cells (FCs), biogas, and energy storage systems (ESSs) are some such alternate sources for power generation (Yang et al. 2021), (Cai et al. 2019). Among all alternate sources, FCs have numerous advantages because of their modular structure that provides improved reliability, flexibility, and scalability to the desired level of power generation (Correa et al. 2004), (Kuan, Chang, and Ku 2017). Additionally, electrolyzers can be used to convert surplus electricity from RES toward hydrogen fuel generation, which can be stored and used to supply power from FCs during power deficient conditions (Ahmadi, Abdi, and Kakavand 2017a). The entire operation of electrolyzers and

CONTACT Ramesh Gugulothu rameshphd@student.nitw.ac.in Department of Electrical Engineering, National Institute of Technology Warangal, Telangana, India

FCs is pollution-free and emits almost zero greenhouse gases, as hydrogen fuel and atmospheric oxygen are used as input and they produce electricity and water as output through a chemical process. FCs has been classified into various types and methodologies, including direct methanol FCs, solid oxide FCs, molten carbonate FCs, proton exchange membrane FCs (PEMFCs), alkaline FCs, and phosphoric acid FCs. Among these, PEMFCs are highly popular due to their superior performance characteristics such as quick start-up, low weight, and optimum working temperature and they can be used for electric vehicles (EV) and residential applications (Zhang, Yan, and Gu 2014), (Benchouia et al. 2015). However methodology for determining acceptable marginal pricing in different locations (Akbary et al. 2019).

In FCs, the output is sensitive to changes in operating temperature (Dargahi et al. 2008), membrane water content (MWC), hydrogen gas pressure, and oxygen pressures (Wang et al. 2016), (Kirubakaran, Jain, and Nema 2009). For a constant temperature, MWC, hydrogen gas pressure, and oxygen partial pressures, PEMFC shows non-linear V – I and P – I characteristics with a global peak power point for varying current as shown in Figure 1(a). Hence, it is desirable to operate FCs at a maximum power point (MPP) to have improved FC efficiency. This paper's primary emphasis is the creation of a heuristic optimization technique to achieve fast-tracking global MPP with reduced oscillations in a steady state.

Similar to photovoltaic and wind turbine systems, the maximum power point tracking (MPPT) methods are required for FC to trace MPP and exhibit improved efficiency at a constant hydrogen pressure and oxygen partial pressures. A Perturb and Observe (P&O) algorithm-based MPPT technique for a grid-connected FC system was detailed in (Egiziano et al. 2009), (Dargahi et al. 2008). Similarly, in (Benyahia et al. 2014) P&O algorithm MPPT was applied to an FC designed for charging EV through a soft switching DC/DC converter. In (Karami et al. 2014) conventional P&O and incremental conductance (INCO) methods were applied for MPPT in FC systems and a comparison is provided; however, the conventional methods exhibited steady-state oscillations around MPP. Further, the INCO-based strategy does not guarantee optimal solution for any sudden or large operational changes. A detailed comparison of P&O, INCO, and incremental resistance (INRE) techniques applied to PEMFCs is presented in (Rezk and Fathy 2020), where INRE exhibited improved tracking responsiveness under a variety of operational scenarios. The P&O and INCO MPPT techniques were also applied in FC-powered EVs (Mohamed, Chandrakala, and Subramani 2019), to improve the vehicle driving range and performance. However, each of these strategies has its own set of limitations. Because of the fixed step size (FSS), P&O oscillates around MPP, resulting in energy loss. Furthermore, because of lower convergence, P&O has been unable to detect MPP in quick changes under high temperature conditions or MWC. The INCO MPPT approach is more complicated than P&O, although it is very useful in coping with sudden changes. However, with FSS, the consequent fluctuations make this approach less efficient.

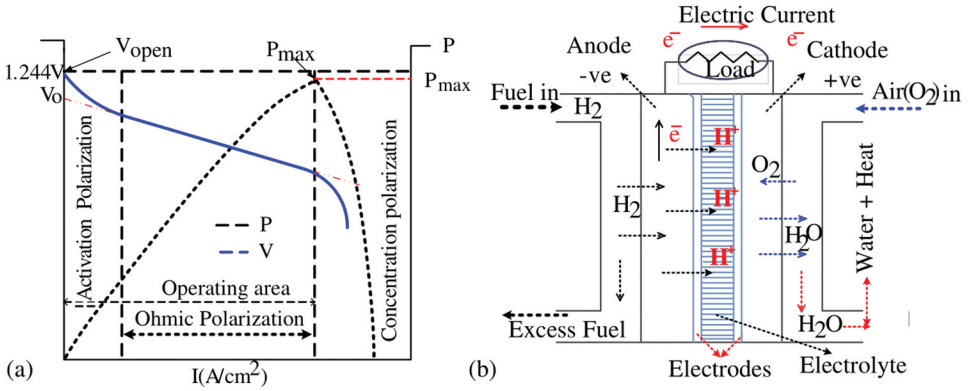

Figure 1. Fuel cell (a) $P - I$ and $V - I$ characteristic (b) Functional diagram.

Further, to reduce the steady oscillation in conventional MPPT technique, recently, an innovative fractional-order INCO technique with variable step size (VSS) was reported (Chen et al. 2017). This approach outperformed P&O and INCO in terms of dynamic, steady-state reactions and can be used with reduced sampling points and without the use of air pressure and moisture measurements, which results in cost savings. It was determined that the MPPT improves FC efficacy as much as traditional techniques by decreasing excessive power loss. To improve the tracking speed and to have MPP operation for a wide range of operating conditions, an artificial neural network (ANN)-based VSS INCO MPPT (Jyotheeswara Reddy and Sudhakar 2018) technique for an FC was developed, but training the ANN is challenging. (Sarvi M 2010) proposed a voltage, and current-based MPPT to decrease FC use, therein exploring the relationship between voltage (Voc voltage) and thus the voltage during MPP; the second investigates the relationship between current (Isc current) and thus the current during MPP. In (Dargahi et al. 2008), FC/BESS system was designed and assessed by providing a P&O algorithm to increase FC generated power. To maximize the overall output power from a PEMFC, a controller design technique comprising implicit model predictive using oxygen over-supply reference regulator was proposed (Li et al. 2013). The findings in (Bizon 2010), shown to be a bidirectional approach, may be used to track the MPP of FC. In (Fathabadi 2016), MPPT was intended to be integrated with a combination of FC/wind approach to enhance the power generated; the efficacy of MPPT used as FC increased to 99.41%. To enhance system effectiveness, the FC power and utilization efficiency were improved using a global extremum searching algorithm (Bizon 2017), while the overall efficiency was raised in the region [1%, 2.1%]. (Bizon, Radut, and Oproescu 2015) offered four control methodologies for regulating the energy of an FC hybrid power generator that increased the total energy of an FC by 12% when compared to standard approaches. (Yang et al. 2017) Enhanced the efficiency of MPPT utilized in FCs using a fractional-order high pass filter. The MPPT integrated with PEMFC was simulated using a water cycle algorithm (WCA) (Nasiri Avanaki I 2016). An optimized fuzzy logic MPPT was developed in (Aly and Rezk 2020), where a meta-heuristic-based differential evolution (DE) technique was used optimally to design the feature set of the fuzzy logic controller to enhance the tracking efficiency, and generate low ripple at peak point for the FC system. However, the DE contains several user-defined parameters (population size, mutation, crossover, etc) and influences membership function. A slap swarm algorithm (SSA) (Fathy et al. 2021) was implemented to get as much power from inside the FC. In this, SSA was used to obtain the estimate of the voltage point corresponding to MPP and then the voltage was regulated using a PID Control strategy for achieving the maximum power of a PEMFC. However, in FCs, the MPPT is made effective through a current controller rather than a voltage controller. However, SSA-PID requires and is not simple to implement in real-time. This is mainly because the peak power characteristics are observed against varying current as seen in Figure 1(a).

To address this, a current estimator using curve fitting technique was used to obtain MPP reference current; the reference current is tracked using high-order sliding control (Derbeli et al. 2020) for fast-tracking MPP in an FC. Sliding control is highly dependent on sliding surface and might cause increased steady-state oscillations. An MPPT depending on an adaptive neuro-fuzzy controller (Reddy and Natarajan 2019a) was also developed to improve the efficacy of PEMFCs used in EVs, but training the neural system and developing fuzzy rules is challenging. Similarly, ANN-based MPPT techniques were proposed for regulating PEMFCs (Harrag and Bahri 2017). In (Mallick and Mukherjee 2020), a modified P&O MPPT algorithm was used in combination with a closed-loop fuzzy logic control to obtain the exact global peak point with reduced steady oscillations. However, extensive data are necessary for training. Other than conventional, ANN, and fuzzy logic-based MPPT techniques, meta-heuristics-based optimization techniques (Harrabi et al. 2018) are widely used for MPPT due to their superior tracking speed and accuracies. In (Ahmadi, Abdi, and Kakavand 2017b), a combined particle swarm optimization (PSO)- PID controller-based MPPT was developed in which the PSO provides the reference current corresponding to MPP point of FCs to the PID controller, which controls the fuel output current tracking MPP. However, in the PSO-PID approach, the PID controller gain tuning is crucial and

plays a vital role in tracking speed. Similarly, Mamdani's fuzzy theory-based and PSO-based MPPT algorithms for FCs are compared in (Luta and Raji 2019). In this, the authors observed that PSO-based MPPT outperformed Mamdani fuzzy-basis MPPT in terms of rising time and overshoot. For instance, a sine-cosine algorithm (SCA) approach was used with PID design in (Shashikant and Shaw 2019) for MPPT tracking. In (Kumar and Shaw 2019), the ant-lion optimizer (ALO) approach was taken into account for constructing the maximum power point PID controller. However, SCA and ALO techniques require more computation time and their implementation poses challenger. For evaluating MPPT of FC-based electric cars, the chicken swarm optimization (CSO) technique was adopted (Priyadarshi et al. 2021). Furthermore, a bi-directional converter with a neutralized zero current controller was fitted to reduce switching operation losses and improve efficiency. Although the given technique outperforms many traditional approaches, the CSO seems to have a poor convergence rate. In (Derbeli, Barambones, and Sbita 2018), an MPPT for a PEMFC is proposed, which depends on estimating the reference current using a backstepped technique to extract optimum power from the fuel cell and a Lyapunov study was carried out to analyze the tracker's reliability. Furthermore, the back movement method converged to MPP under multiple dynamics conditions. (Nasiri Avanaki and Mohammad 2016) presented water cycle algorithms (WCA)-PID MPPT-based technique for PEMFC. WCA is used to calculate the voltage during peak power, while the proportional controller is used to adjust the duty cycle of the boost converter. WCA has its advantages over P&O but MPPT was found to have limitations during the tracking stages. Similarly, a Grey wolf optimizer (GWO)-based optimization was used for tuning PID controller in (Rana et al. 2019) to make FC change in output power to current ratio zero, i.e. to reduce $\frac{dP}{dI} = 0$. Moreover, GWO has poor accuracy and sluggish convergence. An MPPT focused on an adapted neuro-fuzzy intimation system (ANFIS) is described in (Reddy and Natarajan 2019b) to improve the effectiveness of PEM fuel cells used in electric cars. The results showed that ANFIS outperformed traditional fuzzy methods. ANFIS, on the other hand, requires large amounts of data and memory for training. In addition, some new metaheuristic approaches have been included in Table 1

From Figure 1 (a), it is evident that for any given temperature, hydrogen pressure, oxygen pressure, and FC exhibit non-linear hill characteristics. In most literature, FCs are mostly used as dispatchable sources (Agrawal, Samanta, and Ghosh 2021; Ao et al. 2021; Islam et al. 2021; Khan, Ahmad, and Ul Abideen 2019; Kim et al. 2021; Mungporn et al. 2020; Shen, Lim, and Shi 2020; Sorlei et al. 2021; Thounthong and Davat 2010; Torreglosa et al. 2014) without extracting maximum power. In (Samal, Makireddi, and Barik 2018), (Wang et al. 2016), a comparative analysis of MPPT for FC applications against that of without MPPT operation is reported, where the authors showed there can be 94.5% improved efficiency with MPPT. Further, some authors developed advanced MPPT techniques for FC to boost tracking performance and accuracy. The significant performance parameters used to evaluate different MPPT techniques are tracking speed, FC power ripples and variation, computational loads, and implementation complexity. The majority of meta-heuristic MPPT techniques employed PID controller to track peak power point. The use of a PID controller makes the MPPT tracking less efficient as it is highly dependent on PID controller gains.

In this work, the Jaya algorithm-based MPPT tracking technique without a PID controller is developed to achieve the PEMFC's MPP. The proposed approach improves the MPP tracking speed with minimal oscillations for a given value of hydrogen and oxygen pressure. The key contributions of the paper are:

- Development of Meta-heuristic Jaya-based MPPT technique for PEMFCs.
- Designing Jaya algorithm for PEMFCs MPPT without any additional PID controller.
- Detailed comparisons with other methods to show the superiority of the proposed method.
- Hardware realization of the proposed approach considering various real-time disturbances and operating conditions.

Table 1. An overview of some of the methods used to simulate MPPT on PEMFC.

Reference	Period	Approach	Meta-heuristic	Power Converter	Remarks
(Aly and Rezk 2020)	2020	Based on fuzzy inference system Differential evolution	✓	Boost	DE contains several regulating factors (size of population, mutation factor, and crossover consistent) that must be specified by the user.
(Fathy et al. 2021)	2020	SSA-PIDs	✓	Boost	Extensive implementation effort is required.
(Derbeli et al. 2020)	2020	Sliding mode control with high order	✗	Boost	Because SMC is dependent upon that sliding surface, it cannot ensure maximum power.
(Priyadarshi et al. 2021)	2020	Chicken swarm optimizer (CSO)	✓	Bi-directed	The convergence rate of CSO is poor.
(Mallick and Mukherjee 2020)	2020	ANN	✗	Boost	Extensive data is necessary for training.
(Luta and Raji 2019)	2019	PSO- Fuzzy Logic	✓	Boost	PSO has a poor rate of convergence.
(Rana et al. 2019)	2019	GWO-PID	✓	Boost	GWO has poor accuracy and sluggish convergence.
(Mohamed, Chandrakala, and Subramani 2019)	2019	P&O and INCO	✗	Boost	Because of its fluctuation around that, P&O cannot guarantee maximum power.
(Derbeli et al. 2020)	2019	Slide mode rule is based on the PI system.	✗	Boost	Because of the dependence uponthis surface,SMC cannot guarantee maximum power.
(Reddy and Natarajan 2019b)	2019	ANFIS	✗	Boost	ANFIS training needs a large amount of data.
(36)	2019	Sine cosine algorithm (SCA)	✓	Boost	Implementation is challenging.
(Derbeli, Barambones, and Sbita 2018)	2019	Antlion optimizer (ALO)	✓	Boost	Computation timeis excessive.
(Harrag and Messalti 2018)	2018	An technique based on fuzzy logic	✓	Boost	The precision of fuzzy logic is poor.
(Harrabi et al. 2018)	2018	An technique based on fuzzy logic	✓	Buck	The precision of fuzzy logic is poor.
(Raj A 2018)	2018	ANFIS	✓	Boost	ANN need a large amount of data.

The remainder of the paper is organized as follows: Section II explains the modelling, characteristics, and operating principle of the fuel cell. Section III describes the proposed Jaya algorithm to be used for MPPT Tracking of PEMFC. Test system and simulation case studies are detailed in Section IV. Section V provides hardware prototyping and the experimental results under various conditions, and comparative studies with existing methods. Finally, the conclusions are detailed in Section VI.

PEMFC modelling and operation

Fuel cells are energy exchangers that transform chemical energy into electrical energy using Anode $(-ve)$ and Cathode $(+ve)$ electrodes that are separated through an electrolyte. The FC takes hydrogen (H_2) and atmospheric oxygen (O_2) as inputs at the anode and cathode sides, respectively, as shown in Figure 1 (b). At the anode, (H_2) decomposes into protons and electrons given by (1), in which protons $(2H^+)$ move toward the cathode through the catalyst layer, while electrons $(2e^-)$ touch the cathode through an external circuit that links the load (Caisheng Wang, Shaw, and Shaw 2005; Liu, Zhao, and Chen 2017; Pasricha and Shaw 2006; Wang and Nehrir 2007). At the cathode, the protons (H^+) and electrons (e^-) react with atmospheric oxygen and produce water (H_2O) as a by-product as shown in equation (2). Modelling of hydrogen FC storage systems is explained in (Liu et al. 2020). A single FC generates low direct current (DC) power. Hence, many FCs were stacked together in both series-parallel combinations to generate large power with considerable voltage levels. The anode and cathode responses, including the total reactions, are presented below;

At anode

$$H_2 = 2H^+ + 2e^- \tag{1}$$

At cathode

$$\frac{1}{2}O_2(g) + 2H^+ + 2e^- = H_2O \tag{2}$$

Overall reaction.

$$2H_2 + O_2 = 2H_2O + Electricity + Heat \tag{3}$$

Numerical modelling of fuel cell

The PEMFC stack voltage is influenced by hydrogen partial pressure (Ph_2), oxygen pressure (Po_2), FC temperature (T), and MWC (λ_m). Moreover, the single FC voltage shows nonlinear (drooping) characteristics of $V - I$ due to the existence of voltage drop caused by activation, concentration, and Ohmic losses. Considering these drops, the FC output voltage is represented as (Larminie, Dicks, and McDonald 2003).

$$V_{cell} = E_{Nernst} - V_{act} - V_{ohmic} - V_{con} \tag{4}$$

where V_{cell} is FC output voltage, V_{act} is activation drop (due to chemical reaction), V_{con} is concentration loss (due to over flooding of water in the FC catalyst), V_{ohmic} is Ohmic loss (due to internal resistance of the FC). V_{Nernst} is the reversible open-circuit output voltage (thermal-electric potentiality of the cell) of the single-cell, given by (Wang et al. 2016), (Larminie, Dicks, and McDonald 2003):

$$E_{Nerst} = \frac{\Delta G}{2F} + \frac{\Delta S}{2F}(T - T_o) + \frac{RT}{2F}\left[\ln(P_{H_2}) + \frac{1}{2}\ln(P_{O_2})\right] \tag{5}$$

where ΔG is Gibbs free energy in (J/mol), ΔS is the entropy change of value, F is Faraday constant $(96487C)$, R is the universal constant of gas $(8.314/K.mol)$, T is the working temperature of the cell $(343K)$, and reference temperature is $(298K)$. Using standard values of ΔG, ΔS, as well as T_0, V_{Nernst} is simplified as

$$E_{Nernst} = 1.229 - 8.5 \times 10^{-4}(T - 298.15) + 4.308 \times 10^{-5}(\ln(P_{h_2}) + 0.5\ln(Po_2)) \tag{6}$$

The activation voltage drop V_{act} is given as (Egiziano et al. 2009)

$$V_{act} = [\xi_1 + \xi_2 T + \xi_3 T ln(C_{O_2}) + \xi_4 T ln(I_{FC})] \tag{7}$$

where, $\xi_i (i = 1 - 4)$ are the characteristic coefficients of FC; CO_2 (atm) is the oxygen concentration in (mol cm^{-3}) given by (8) and I_{FC} is FC current.

$$CO_2 = \frac{P_{O_2}}{(5.08 \times 10^6) \times \exp(-498/T)} \tag{8}$$

V_{ohmic} is Ohmic over-voltage drop obtained as follows

$$V_{ohmic} = I_{FC}(R_M + R_C) \tag{9}$$

V_{ohmic} of the FC can be minimized using conductive materials and an electrolyte membrane. R_C in (9) is the lead contact resistance, which is assumed to be constant as it is independent of FC working temperature. R_M is the resistance of the PEM and is represented by an empirical formula;

$$R_M = \frac{r_m t_m}{A} \tag{10}$$

$$r_m = \frac{181.6\left[1 + 0.03(I_{FC}/A) + 0.0062(T/303)\left((I_{FC}/A)^{2.5}\right)\right]}{[\lambda_m - 0.634 - 3(I_{FC}/A)]\exp[(4.18(T - 303/T))]} \tag{11}$$

Here, r_m is the resistance of the electrolyte membrane in $(\Omega.cm)$, $t_m = (0.0178cm)$ is the thickness of the electrolyte membrane, $A = 232(cm^2)$ is the activation area of the FC, λ_m is MWC with a typical value range in $(0 - 14)$ with a relative humidity of 100%.

The voltage loss V_{con} due to over flooding of water in the FC catalyst is given by:

$$V_{Con} = -\frac{RT}{nF} * \ln\left(1 - \frac{I_{FC}}{i_L A}\right) \tag{12}$$

where n is the number of electrons contained in the reaction,i_L indicates limiting current and R is the gas universal constant. The overall output voltage and power of the stacked FC are obtained thus:

$$V_{FC} = N_{FC} V_{cell} \tag{13}$$

$$P_{FC} = V_{FC} I_{FC} \tag{14}$$

where$(N_{FC} = 35)$ is the total number of FCs, $(V_{FC}), (I_{FC}),$ and (P_{FC}) are the output voltage, current, power of the FC stack, respectively.

In ideal conditions, the fuel cell has three different regions, (i) active polarization, (ii) ohmic polarization, and (iii) concentration polarization. A combination of three regions results in polarization curves and the curves have three different characteristics in $V - I$ curves as shown in Figure 1 (a). The electrical energy is extracted from FC only if the current is absorbed by the loads which in turn results in a drop in FC voltage due to irreversible loss mechanisms. Ideally, the ohmic polarization curve region exhibits inverse slope characteristics in which the FC is operated. The extension of the ohmic polarization line toward zero current gives open-circuit voltage V_o. From the ohmic polarization region, it is clear that power rises with an increase in current and reaches a peak and then the operation reaches the concentration region in which power decreases with increased current (as in Figure 1).

Further, the $V - I$ and $P - I$ curves are sensitive to FC parameters such as temperature (T), WMC (λ_m), hydrogen partial pressure (Ph_2), and oxygen pressure (Po_2). Figure 2 portrays FC $P - I$ and $V - I$ curves for (T) is varying keeping λ_m, Ph_2 and Po_2 are constant. Similarly, the FC characteristics under varying MWC (λ_m), hydrogen gas pressure Ph_2 with other parameters being constant are shown in Figure 3, and Figure 4, respectively. All the curves show that the FC output power is a nonlinear function of current and the curves are highly affected by cell temperature, MWC, hydrogen gas pressure, and oxygen pressure.

A fast and accurate MPPT technique is required to regulate FC current so that maximum possible power can be extracted for any FC parameter variation. Thus, in this paper, a Jaya-optimization-based MPPT control is developed to ensure MPP operation in the Ohmic region.

Constructing a DC-DC converter

Fuel cells are usually connected to the DC bus through a DC/DC boost converter to ensure regulated output voltage, irrespective of load demand. The step-up interleaved converter (Ye et al. 2020) is also designed to ensure FC operation in the linear domain of $V - I$ characteristics as there is a possibility of damage to the electrolyte membrane when operated in non-linear region of $V - I$ characteristics. Figure 5 portrays the closed-loop DC/DC converter (Cha et al. 2006). The parameters of the power converter are tabulated in 5. The duty of the converter is controlled using the maximum power tracking controller. The output voltage for varying duty (d) is given by (15);

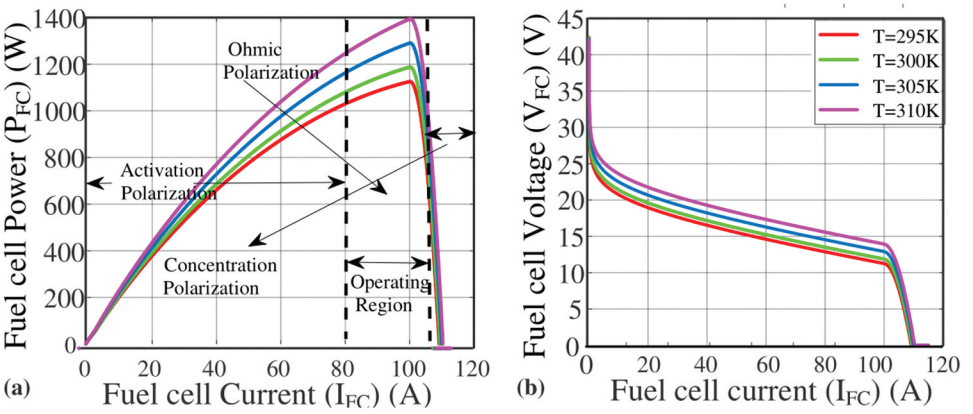

Figure 2. $P - I$ and $V - I$ curves at various fuel cell temperatures

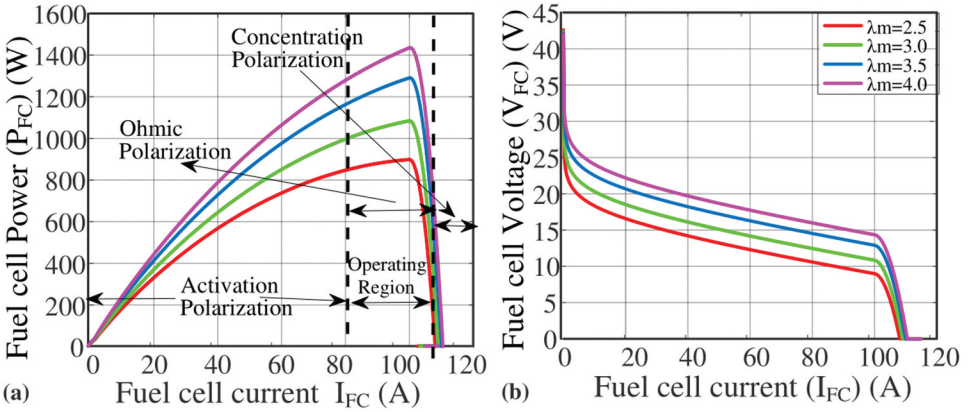

Figure 3. Variation in fuel cell water content affecting $P - I$ and $V - I$ curves.

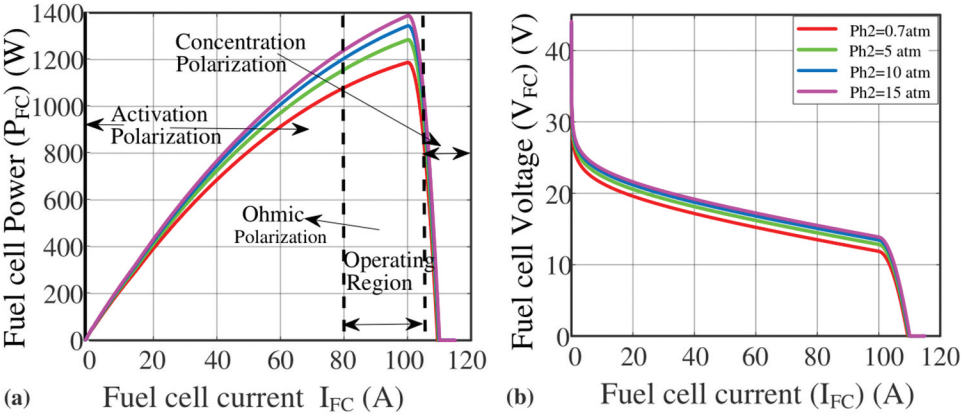

Figure 4. $P - I$ and $V - I$ curves of a fuel cell at various hydrogen gas pressures

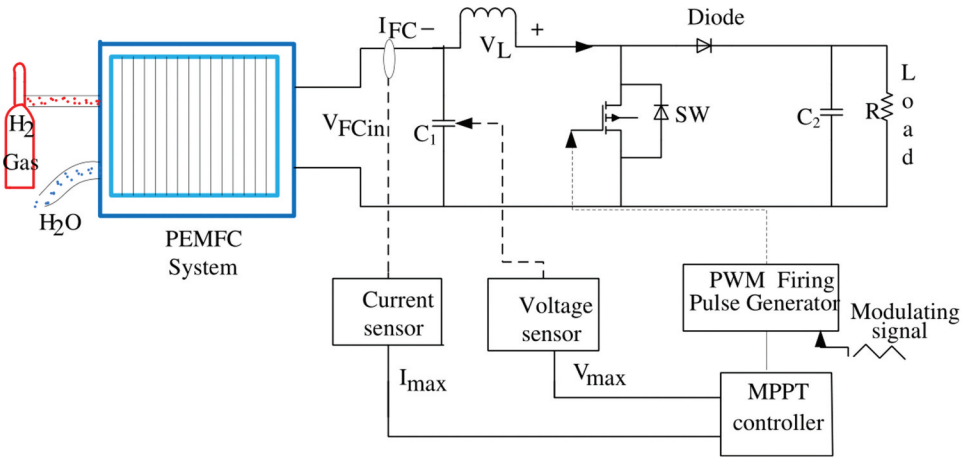

Figure 5. Block diagram of the proposed system setup.

$$\frac{V_o}{V_{FC}} = \frac{1}{1-d} \tag{15}$$

Where V_{FC}, V_o, are the input, and output voltages, d is the duty ratio.

MPPT algorithm

As explained before, the MPP of the FC changes within FC variables such as T, Ph_2, Po_2, and λ_m. By using MPPT methods, one can find an optimal current and voltage operating point that can be obtained so that it has maximum output power with high efficiency for a given system. In this paper, a Jaya-based MPPT has been developed for an FC system with such a boost converter coupled to the resistive load as shown in Figure 5.

MPPT through proposed Jaya algorithm

Jaya method is a recently developed meta-heuristic technique for addressing restricted complicated non-convex optimization problems (Bhukya and Nandiraju 2020). This method is different compared to other heuristic techniques as it takes only two popular parameters, namely, "number of iterations" and "population size" as inputs, and the parametric values can be easily initialized for any optimization problem making the utilization of Jaya algorithm simple and convenient.

The power output P_{FC} is considered as the objective function in the MPPT tracking of the FC. Initially, a random population set $D = \{d_1, d_2, \ldots d_n\}$ of size 'n' corresponding to the duty cycle is generated. For a set of duty cycles D, the power output P_{FC} is obtained from FC measurements. Two intermediate variables, d_{best} and d_{worst} are defined to which the best and worst function valued candidates are assigned, respectively (Venkata Rao 2016), (Huang et al. 2018). In each iteration, the population set is updated using the best and worst candidates. In the Jaya algorithm shown in Figure 6, the update rule of i^{th} candidate in k^{th} iteration is given by:

$$d_i^{k+1} = d_i^k + r_1\left(d_{best} - d_i^k\right) - r_2\left(d_{worst} - d_i^k\right) \tag{16}$$

$$d_i^{k+1} = \begin{cases} d_i^{k+1}, iff\left(d_i^{k+1}\right) > f\left(d_i^k\right) \\ d_i^k, iff\left(d_i^{k+1}\right) \le f\left(d_i^k\right) \end{cases} \tag{17}$$

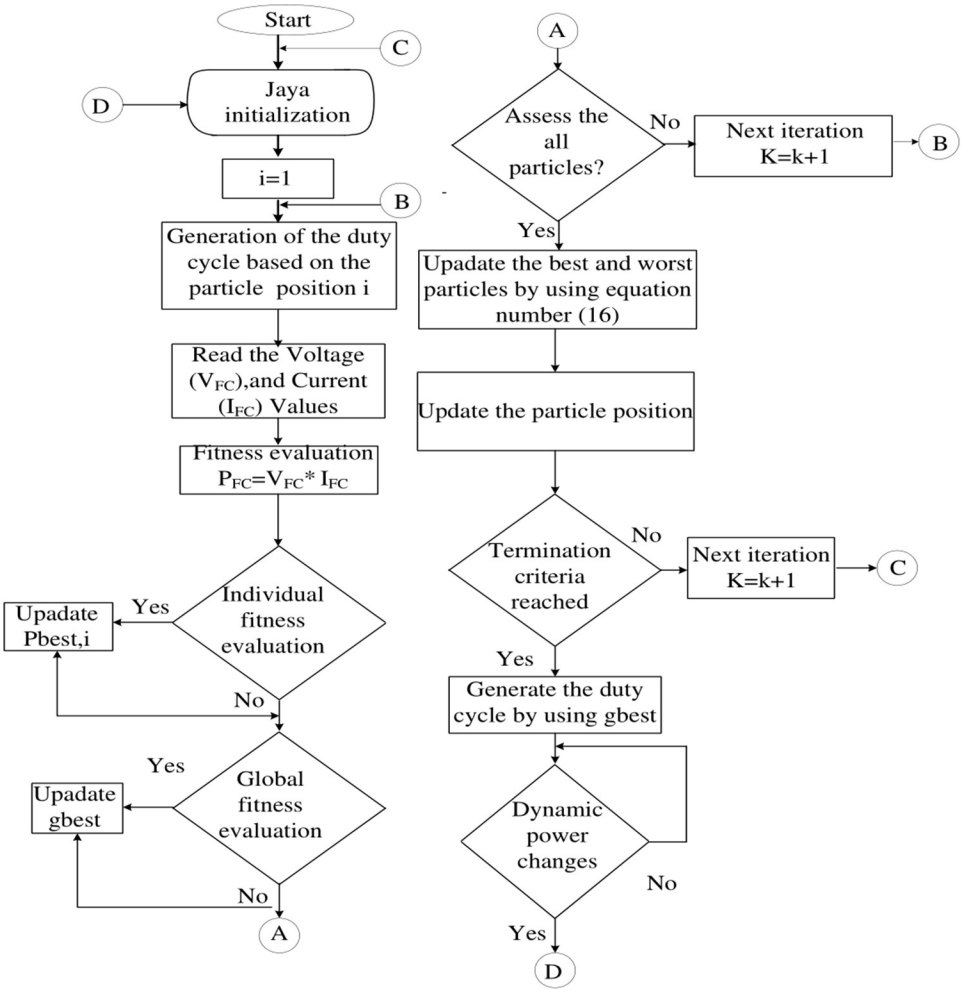

Figure 6. Jaya optimization algorithm for fuel cell.

where d_i^k and d_i^{k+1} represent the actual and upgraded values, d_{best} and d_{worst} represent the best and worst responses across all the candidates with r_1 as well as r_2 being random numbers between $U[0, 1]$. The expression $r_1\left(d_{best} - d_i^k\right)$ refers to the solution that is closest to the best, while $r_2\left(d_{worst} - d_i^k\right)$ refers to the worst solution to be avoided. The termination process is met if the maximum proportion of iterations is achieved or the difference between $|d_{best} - d_{worst}| < \in$. As shown in algorithm 1.

Algorithm 1 Jaya optimization based MPPT tracking.

1: while $iter_{count} < iter_{max} do$
2: initialize n, random set D $=\{d_{1,}d_{2,\ldots.}d_{n,}\}$, $iter_{max,}$ $iter_{count}$
3: obtain $P_{FC} = \{P_{FC}(d_i) \quad i = 1, 2, \ldots, n\}$
4: assign $d_{best} = \{d \epsilon P_{FC}(d) = max(P_{FC})\}$ and $d_{worst} = \{d \mathrm{n} P_{FC}(d) = min(P_{FC})\}$
5: update D using (16) and (17)
6: $iter_{count}$ $=iter_{count+1}$
7: return (d_{best})

Simulation results

The proposed method is implemented for the fuel cell system designed in MATLAB/Simulink domain. The FC system includes 35 FCs linked in series, a DC/DC converter, resistive load, and a maximum power tracker. To evaluate the tracking performance and steady-state behavior of the FC system using the proposed Jaya algorithm MPPT method, it is compared with traditional P&O technique and meta-heuristic-based PSO MPPT techniques by performing various case studies under different operating conditions and perturbations given below.

Case-1: MPPT Tracking for constant fuel cell parameter with $(T = 300K)$, $(\lambda_m = 3)$, $(Po_2 = 0.8atm)$, and $(Ph_2 = 0.7atm)$ being constant.

Case-2: Change in the membrane water content (λ_m).

Case-3: Variation in fuel cell temperature (T).

Case-4: Hydrogen gas Partial pressure (Ph_2), and oxygen partial pressure (Po_2) perturbation.

Case-5: Fluctuation in fuel cell temperature (T), membrane water content (λ_m), and hydrogen gas partial pressure all occur at the same time (Ph_2).

Case-1: MPPT Tracking for constant fuel cell parameter with $(T = 300K)$, $(\lambda_m = 3)$, $(Po_2 = 0.8atm)$, and $(Ph_2 = 0.7atm)$ being constant.

In this study, fuel cell temperature $(T = 300K)$, MWC $(\lambda_m = 3)$, hydrogen gas pressure $(Ph_2 = 0.7atm)$, and oxygen partial pressure $(Po_2 = 0.8atm)$ determined and kept constant. The respective $P - I$ and $V - I$ behavior of FC system are shown in Figure 7 for the system parameters; MPPT tracking using the proposed Jaya algorithm, PSO, and P&O techniques is shown in Figure 8. From the figure, it is noticed that the P&O algorithm took considerable time to track MPP, and persistent oscillations were recorded using this algorithm due to three-step variation around the peak point. Although the MPPT using PSO showed a better steady-state behavior unlike P&O, the transient behavior at the time of MPP tracking the system behavior was oscillatory, as shown in Figure 8, However, the proposed Jaya algorithm-based MPPT showed better transient and steady-state behavior compared to other two methods. A detailed comparative evaluation is given in Table 2.

Case-2: Change in the membrane water content (λ_m).

In this scenario, fuel cell parameters such as hydrogen gas pressure $(Ph_2 = 0.7atm)$, oxygen pressure $(Po_2 = 0.8atm)$, and temperature $(T = 300K)$ are kept constant at the given values, while there is variation in MWC. The variation in (λm) concerning time is shown in Figure 9(a) in which WMC is $\lambda_m = 2.5$, and at $t = 1.5s$, the MWC of the cell is assumed to be 3.5 and held at that value till $t = 3s$, after which MWC attains a value of 2.5, and then is held constant for the rest of the simulation period. Figure 9(b) portrays the Jaya algorithm-based MPP tracking process on an FC $P - I$ curve when the

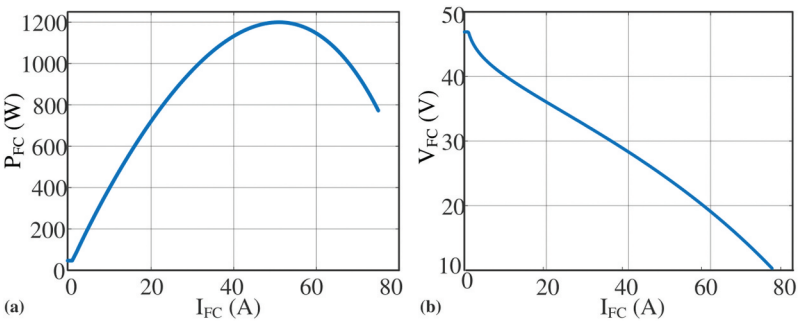

Figure 7. Fuel cell characteristics at $T = 300K$, $\lambda_m = 3$, $Po_2 = 0.8atm$, $Ph_2 = 0.7atm$, (a) P – I curve and (b) V – I curve.

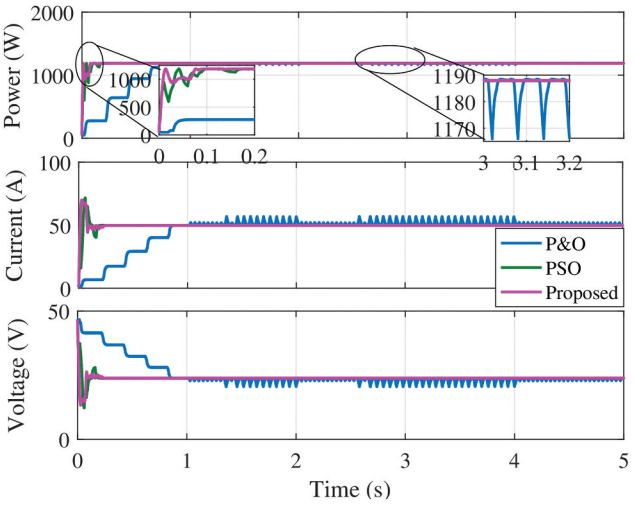

Figure 8. MPPT tracking of power, current, and voltage in normal operating conditions for the proposed technique, PSO, and P&O techniques.

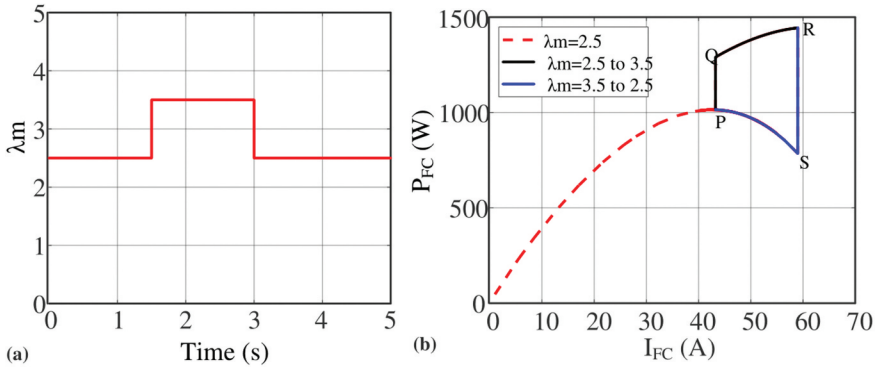

Figure 9. Tracking the P − I characteristics of a fuel cell as water content changes (a) water content variation (b) tracing the $P-I$ curve as the water content varies.

MWC is varied. Initially, when the MWC is at $\lambda_m = 2.5$, the FC is operating at MPP point P; later, when the MWC is suddenly changed from $2.5to3.5$, the operating point shifts from $PtoQ$; however, as Q is not an MPP, Jaya algorithm moves the operating point from $QtoR$ making it operate at MPP when MWC is brought back to $\lambda_m = 2.5$. The operating point shifts to a new point R from S and as S is not an MPP, Jaya algorithm tracks the MPP point and shifts operation back to point P as shown in Figure 9 (b) Accordingly, the time responses of the output power, current, and voltage using Jaya algorithm, PSO, and P&O MPPT techniques are displayed in Figure 10. From the figure, it can be observed that the proposed method has better time response, as well as tracking time as shown in Table 2.

Case-3: Variation in fuel cell temperature (T)

In this scenario, fuel cell parameters such as hydrogen gas pressure ($Ph_2 = 0.7atm$), oxygen partial pressure ($Po_2 = 0.8atm$), and MWC ($\lambda_m = 3$) are kept constant at given values while there is variation in FC temperature. The variation of (T) with time is shown in Figure 11.(a) in which, the initial temperature is considered as $T = 300K$, and at $t = 1.5s$, the temperature of the cell is increased to $340K$ and

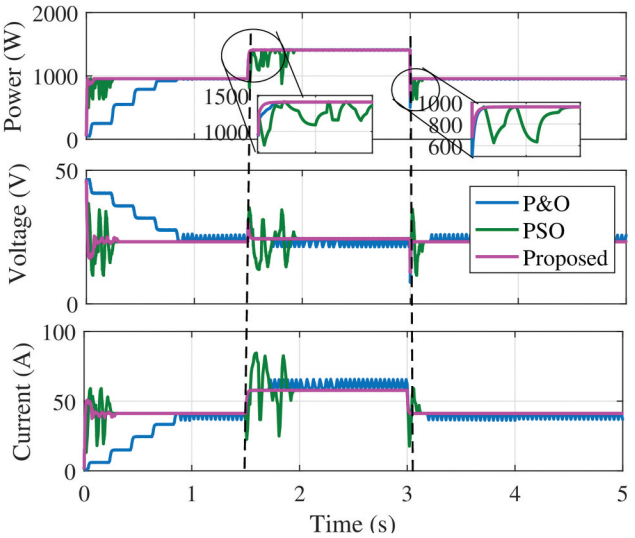

Figure 10. MPPT power, voltage, and current tracking for the proposed, PSO, and P&O systems with significant water content deviation.

maintained at that value till $t = 2.5s$, after which the temperature is ramped down with a slope for up to $t = 5s$ till the temperature reaches $300K$, and remains so for the rest of the simulation time. Figure 11.(b) portrays the Jaya algorithm-based MPP tracking process on an FC $P-I$ curve when the temperature is varied. Initially, when the temperature changes from $T = 300to340K$, the new MPP operating point changes from *PtoR* using Jaya algorithm, shown in Figure 11. (b) Accordingly, the time response of the output power, current, and voltage using Jaya algorithm, PSO, and P&O MPPT techniques is displayed in Figure 12. From the figure it can be observed that the data matches what is shown in Table 2.

Case-4: Hydrogen gas partial pressure (Ph_2), and oxygen partial pressure (Po_2) perturbation

This scenario deals with two different cases, one where hydrogen gas pressure (Ph_2), is constant; in this case, FC parameters such as , $Po_2 = 0.8atm$, $\lambda_m = 3$, and $T = 300K$ are kept constant at given values expect hydrogen gas pressure of the FC Ph_2, and, in case-4 (ii), oxygen partial pressure Po_2 is kept constant; $Ph_2 = 0.7atm$, $\lambda_m = 3$, and $T = 300K$ are held constant at the given values expect the oxygen pressure Po_2 of FC. The variation in FC Ph_2, with respect to time, is shown in Figure 13(a) in which, initial hydrogen gas is considered as $Ph_2 = 0.7atm$, and at $t = 1.5s$, the pressure of hydrogen gas of the cell is increased to $5atm$ and held at that value till $t = 3s$; for case-4 (Po_2) the initial pressure of oxygen gas is taken as $Po_2 = 0.8atm$, and at $t = 1.5s$, the oxygen gas of the cell is increased to $5atm$ and held at that value till $t = 3s$. The MPPs for partial pressure of hydrogen gas are determined by Jaya algorithm which tracks the MPP point and shift operation as shown in Figure 13(b). The workings of the proposed Jaya algorithm, PSO, and P&O MPPT techniques are displayed in Figure 14, when oxygen partial pressure changes as shown in fig.14, in Table 2.

Case-5: Fluctuation in fuel cell temperature (T), membrane water content (λ_m), and hydrogen gas partial pressure all occur at the same time (Ph_2).

In this scenario, the parameter Ph_2, λ_m, and T are changed during the period of $1.5sto3s$ as shown in Figure 13(a). The temperature is changed from $300to340K$, while the variation in Ph_2 and λ_m, is considered as similar to earlier case studies. The sudden changes in the given parameters impact FC MPP; consequently the time response of the output power, current, and voltage using the proposed

Jaya algorithm, PSO, and P&O MPPT techniques are displayed in Figure 15. The P&O shows transient behavior during the MPP tracking, while the system behavior is oscillatory as shown in Figure 15. A detailed comparative evaluation is given in Table 2.

Table 2. Comparison of simulation control approaches with output power, tracking time, and number of iterations of the fuel cell under different conditions.

Cases	Control methods	Rated Power, W	Maximum tracking power, W	Maximum tracking voltage, V	Maximum tracking current, A	Tracking time (s)	Number of iteration required to reach the MPP	Efficiency (%)
Case-1	Without MPPT	$MPP = 1.2KW$	980	25.01	39.22			81.6
	P&O		1113.42	23.1	48.2	0.8		92.78
	PSO		1125.2	23.2	48.5	0.18	6	93.76
	Proposed		1189.7	23.8	49.99	0.12	4	99.14
Case-2	Without MPPT	$MPP = 1.42KW$	1222.21	27.1	45.1			86.07
	P&O		1370.4	24.0	57.1	0.8		96.50
	PSO		1376.11	24.1	57.1	0.445	15	96.90
	Proposed		1411.02	24.37	57.9	0.04	2	99.36
Case-3	Without MPPT	$MPP = 1.8KW$	1604.5	28.1	57.1			89.13
	P&O		1665.31	24.1	69.1	0.75		92.51
	PSO		1743.84	25.2	69.2	0.14	5	96.88
	Proposed		1785.6	25.3	70.58	0.04	2	99.20
Case-4 (Ph_2 changes)	Without MPPT	$MPP = 1.24KW$	1134	27.01	42.01			91.45
	P&O		1141.93	23.3	49.01	0.81		92.09
	PSO		1189.44	23.6	50.4	0.14	5	95.92
	Proposed		1233.94	23.96	51.5	0.045	2	99.51
Case-4 (PO_2 changes)	Without MPPT	$MPP = 1.22KW$	1101.65	27.5	40.06			90.29
	P&O		1127.98	23.02	49	0.82		92.45
	PSO		1139.04	22.6	50.4	0.13	5	93.36
	Proposed		1211.73	23.9	50.7	0.04	2	99.32
Case-5(All variations)	Without MPPT	$MPP = 2.26KW$	1822.4	27.2	67			80.63
	P&O		2100	26.25	80	0.81		92.92
	PSO		2192.4	26.1	84	0.12	4	97.00
	Proposed		2259	26.15	86.4	0.04	2	99.95

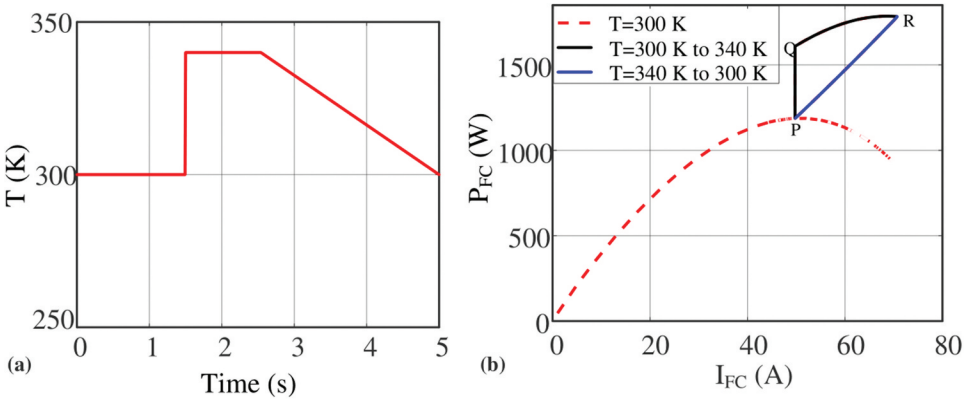

Figure 11. Tracking $P - I$ characteristic of a fuel cell as temperature varies (a) temperature variation (b) tracing the $P - I$ curve as temperature changes.

Experimental results and analysis

The hardware prototype was developed using a fuel cell simulator linked to a power converter that provides a resistive load. The MPPT algorithm along with the converter control was realized through rapid prototype controller dSPACE (DS1104) which was interfaced through MATLAB/SIMULINK. The dSPACE reads the system information through analog inputs taken from the current sensor $(LA55-p)$, and voltage sensor $(LV25-p)$, which are connected at system measuring points. ThiswasdonethroughanFCsimulator(Magnapowersimulator $(XR600-9.9/415+PPPE+HS)$. The complete hardware prototype model is shown in Figure 16 whose system electrical parameters are similar to simulation parameters given in Table 5. The FC simulator is loaded with a few predefined $P-I$ characteristics which are used for all case studies. To assess the efficiency of the proposed MPPT tracking scheme for FCs, two different scenarios were implemented in hardware as shown below:

Scenario-1:MPPTTrackingforConstantFuelcellParameter $(T=300K, Ph_2=0.81atm, Po_2=0.85atm)$.

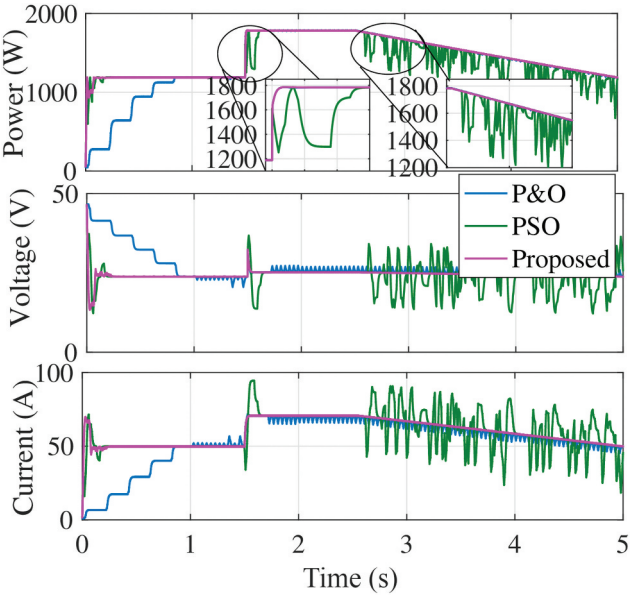

Figure 12. MPPT tracking of power, voltage, and current under sluggish cell temperature variation for the proposed technique, PSO, and P&O techniques.

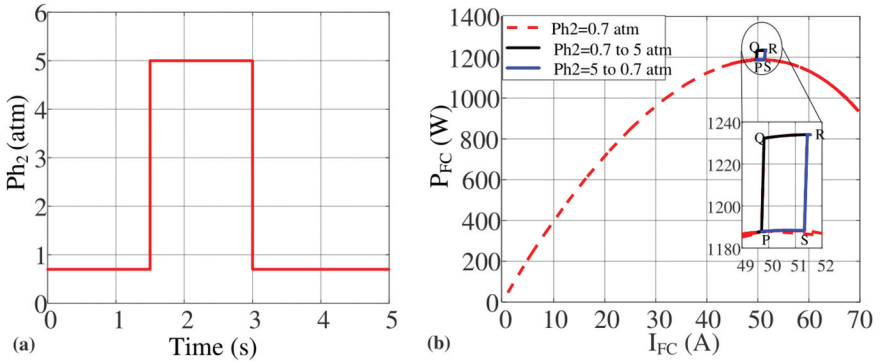

Figure 13. Fuel cell $P-I$ characteristic tracing change in hydrogen pressure. (a) hydrogen pressure variation (b) tracing the $P-I$ curve as hydrogen levels vary pressure.

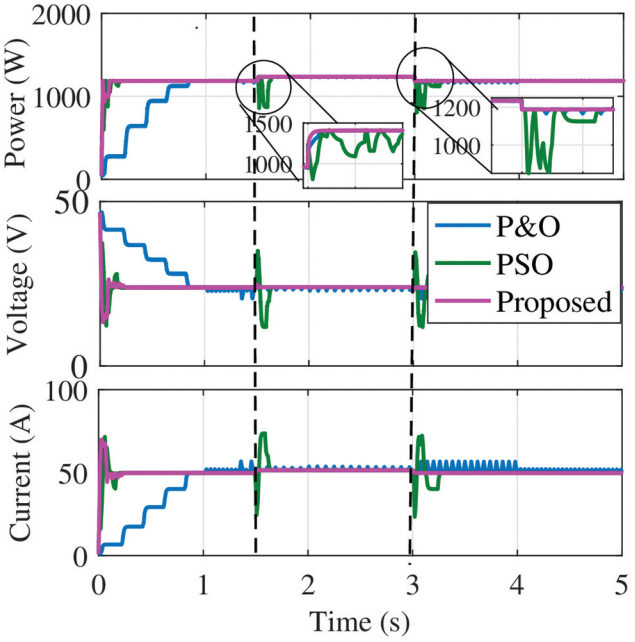

Figure 14. MPPT tracking of power, voltage, and current under quick deviations in hydrogen gas partial pressure for the proposed technique, PSO, and P&O techniques.

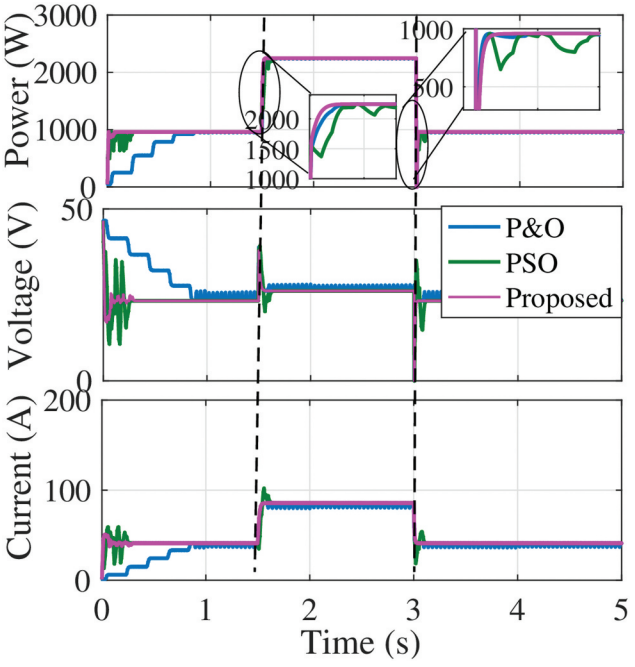

Figure 15. MPPT tracking of power, voltage and current under fast change of fuel cell temperature, water content, hydrogen gas partial pressure, and oxygen partial pressure for proposed, PSO, and P&O Techniques.

Scenario-2: Dynamics in Fast deviation of fuel cell temperature from $(T = 340to300K)$, hydrogen gas partial pressure $(Ph_2 = 0.7atm)$, and oxygen partial pressure $(Po_2 = 0.8atm)$, are kept constant.

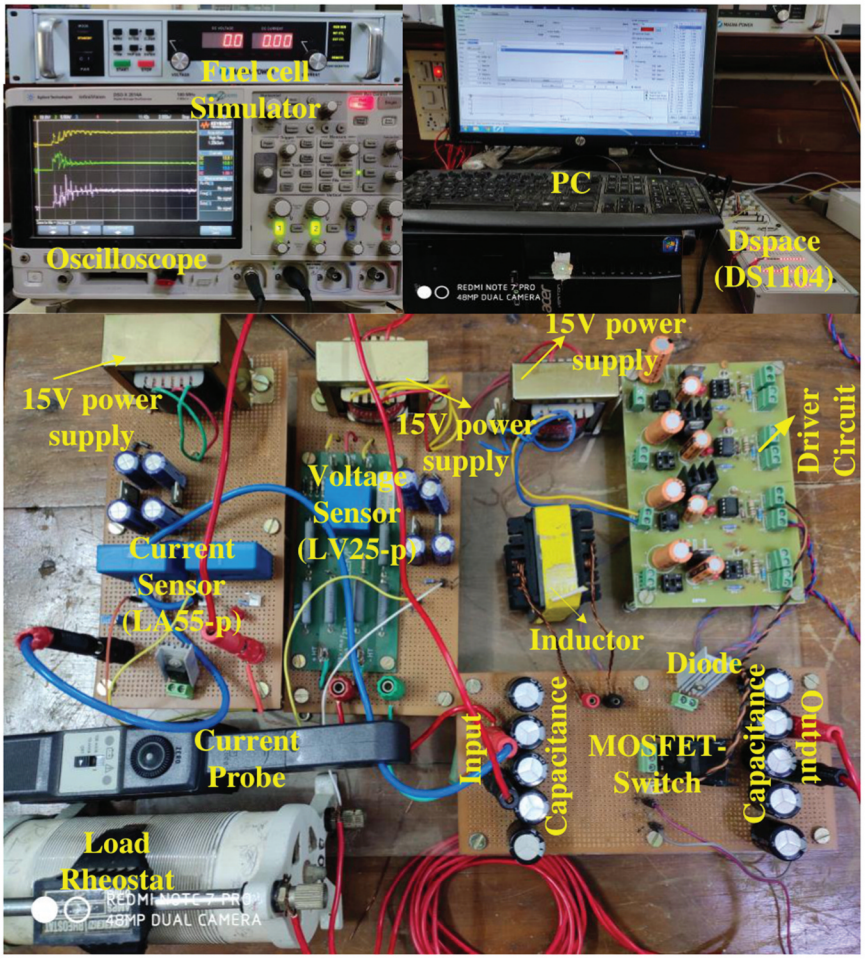

Figure 16. Experimental structure of the established fuel cell system.

Scenario-1: MPPT Tracking for constant fuel cell parameter ($T = 300K$, $Ph_2 = 0.81atm, Po_2 = 0.85atm$)

In this scenario, fuel cell $T = 300K$, $Ph_2 = 0.81$ atm, and $Po_2 = 0.85atm$ are considered at normal operating conditions. For the FC parameters, it is observed that the MPP of the FC curve with maximum power is $98.4W$. The time response of such fuel cell tracking output utilizing P&O, PSO, and the proposed approach, even as it approached maximum point, is illustrated in Figure 17.The P&O algorithm has fluctuating power and can monitor a mean maximum power of $79.9W$ with a tracking duration of $6s$ in steady state condition, as illustrated in Figure 17. The PSO-based MPPT technique is capable of extracting maximum power of $83.3W$ within 4 iterations with a tracking period of $4s$, with significantly decreased steady-state oscillations than P&O but significantly higher transient oscillations when tracking the MPP, as shown in Figure 17.The proposed approach is the ability to extract an average maximum output power of $85.85W$, which is slightly higher than PSO, and track MPP within 3 iterations with a tracking time of $1.75s$, as shown in Figure 17. An analytic comparison of all three MPPT methods for this scenario is provided in Table 3.

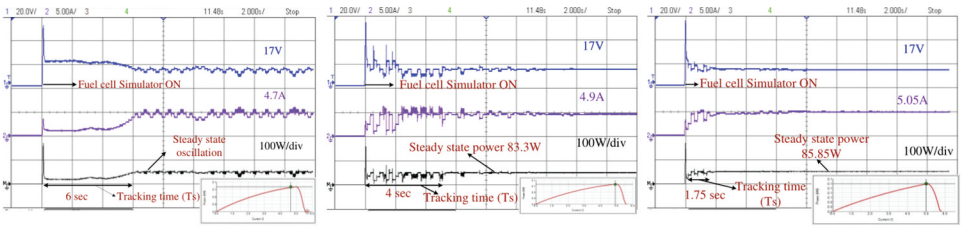

Figure 17. Experimental results under normal operating conditions.

Table 3. Comparison of three control approaches utilizing experimental data of output power, tracking time, and number of iterations of the fuel cell under different conditions.

Scenario	Control Methods	Rated Power, W	Maximum Tracking Power, W	Tracking Time, s	Number of iterations	Efficiency (%)
Scenario-1 Normal condition	P&O	98.4	79.9	6	–	81.19
	PSO		83.3	4	4	84.65
	Proposed		85.85	1.75	3	87.24
Scenario-2 Fast deviation of Temperature $(T = 340K)$	P&O	127	112.5	0.9	–	88.58
	PSO		116.84	4	7	92
	Proposed		117.5	3.5	5	92.51
Scenario-2 Fast deviation of Temperature $(T = 300K)$	P&O	98.4	84	0.9	–	85.36
	PSO		84	3.5	6	85.36
	Proposed		8.65	2	3	86.99

Scenario-2: Dynamics in fast deviation of fuel cell temperature$(T = 340to300K)$.

In this scenario, we applied sudden deviation of FC temperature for verification of the proposed Jaya algorithm on FC system.Figure 18 (a) shows the temperature of FC. The change in temperature proceeded from point P. The sudden temperature change $(T = 340to300K)$ at the operating point changes from $PtoQ$ and as Q is not an MPP, Jaya algorithm tracks the MPP point and shifts operation point to R at a maximum power of $(127W, and 98.4W)$ as shown in Figure 18 (b). To trace the maximum output for a sudden changing in temperature condition, P&O, PSO, and the proposed Jaya algorithm are employed continually to achieve the maximum powers for these methods are $(112.5W, 116.84W, and 117.5W)$; the tracking times are $(0.9s, 4s, and 3.5s)$. There were high changes in FC temperature, the algorithm re-initialized the parameters and updated

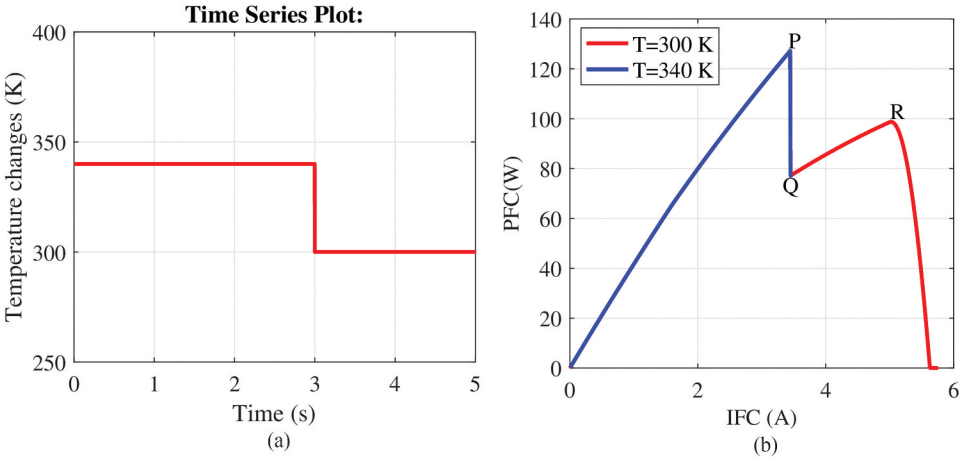

Figure 18. Experimental fuel cell characteristics as a function of temperature (a) Temperature variation (b) P – I curve.

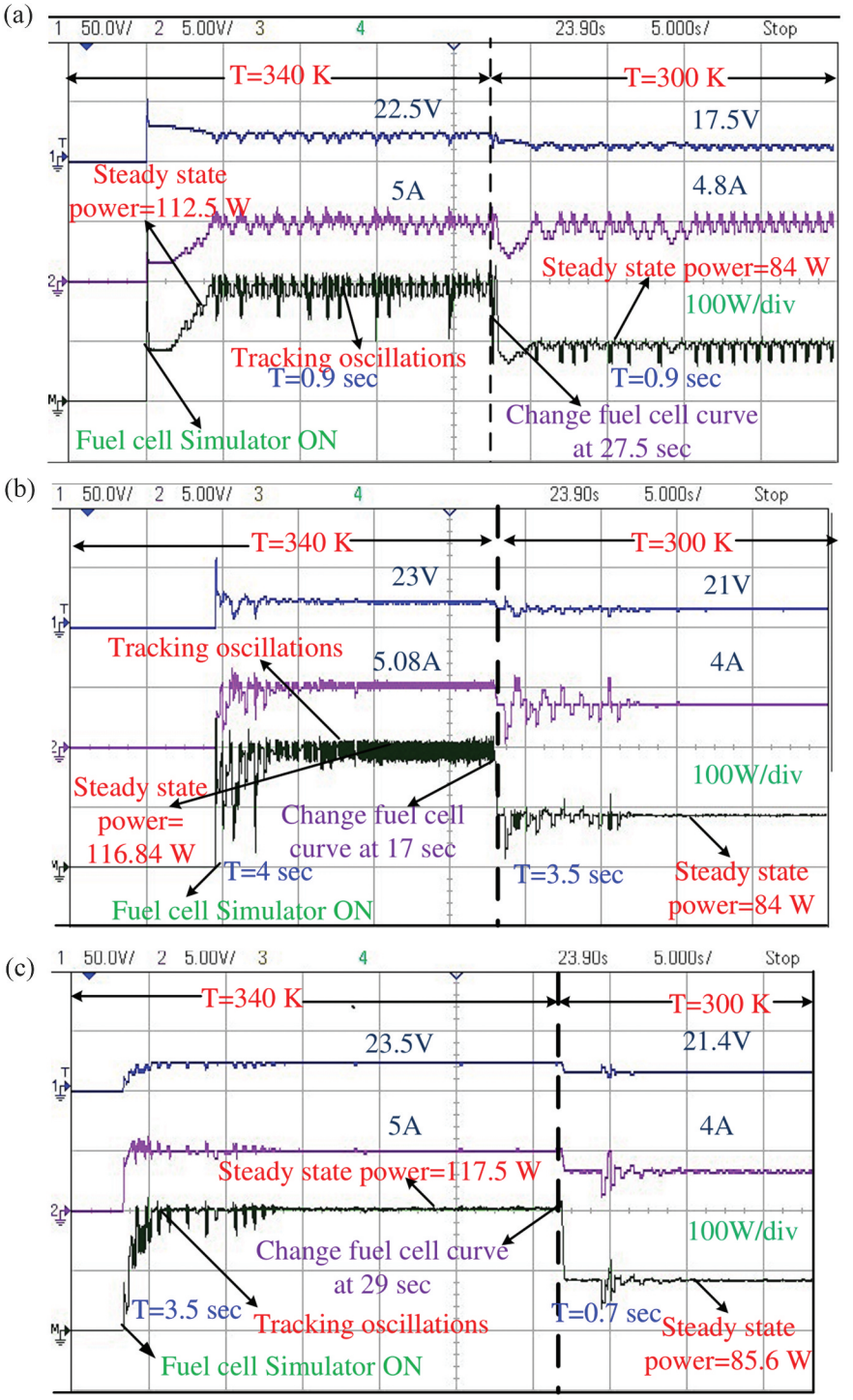

Figure 19. Experimental results with a fast variance of fuel cell temperature (a) P&O (b) PSO (c) proposed.

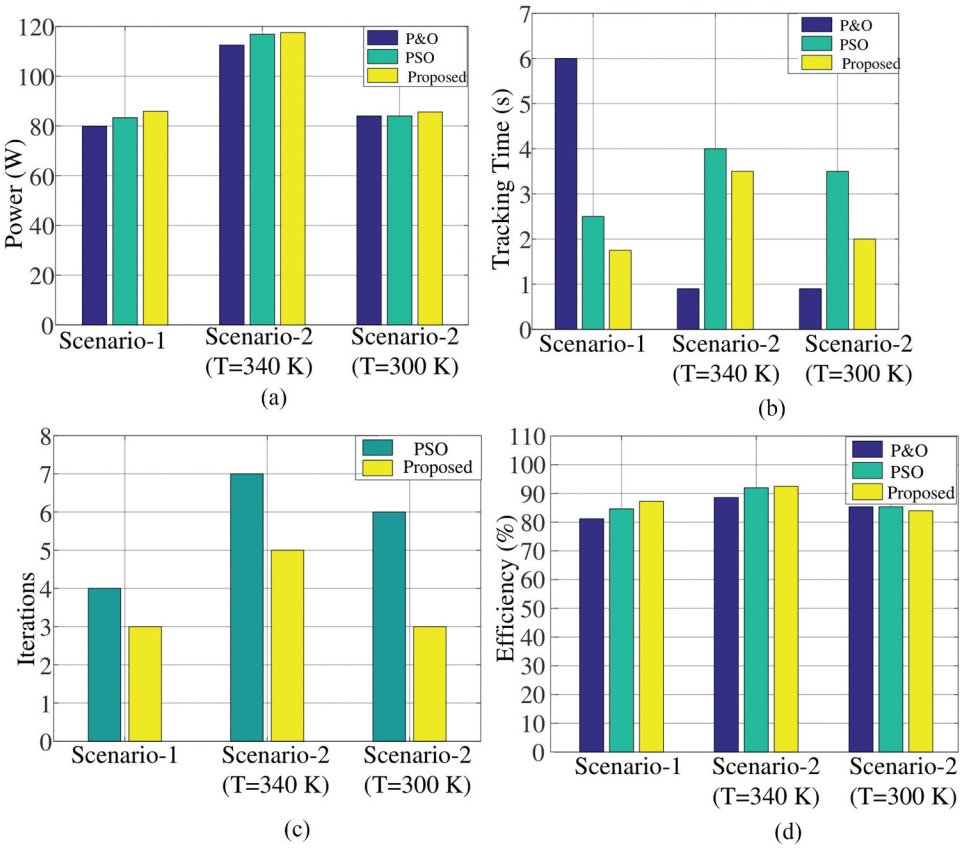

Figure 20. Comparative studies for (a) power (b) tracking time (c) iterations (d) efficiency.

Table 4. Comparison of the proposed Jaya algorithm with existing MPPT.

Variables /Technique	P&O- INCO (Mohamed, Chandrakala, and Subramani 2019)	Fuzzy-PSO (Luta and Raji 2019)	ANFIS (Reddy and Natarajan 2019b)	GWO-PID (Rana et al. 2019)	SSA (Fathy et al. 2021)	Proposed Jaya algorithm
Tracking level	Fast	Moderate	low	Moderate	Fast	Fast
Iterations	Nil	>5	>5	3	3	<3
Tuning parameters	Nil	5	3	2	1	Nil
Initial particles	Dependent	Independent	Independent	Dependent	Dependent	Independent
Efficiency	Moderate	High	High	High	High	Very High

Table 5. Parameters of the proposed method and boost converter.

Particulars	Specifications
PSO	$C_{1min} = C_{2min=1;}C_{1max} = C_{2max} = 2, W_{min}$=0.1,$W_{max} = 1$
Jaya	Maximum iteration = 100, population size = 3.
Incremental conductance	*Dinitial* = 0.15, *DeltaD* = 0.0051.
Boost converter	$L = 0.4mH, C_{in} = C_{out} = 100\mu F, F_s = 10kHz$, VariableRheostat load:100 Ω, 10A.
Sampling period (*Ts*)	For simulation $Ts = 10ms$, For Experimental $Ts = 200ms$.

the new power values of $(84W, 84W, and 85.6W)$ with a tracking time of $(0.9s, 3.5s, and 2s)$. Accordingly, the time response of power output, current, and voltage using the proposed Jaya algorithm, PSO, and P& O MPPT techniques are displayed in Figure 19. It is evident from the data

that the proposed Jaya algorithm is superior to other algorithms. The comparative charts for the above two cases in terms of power, tracking time, iterations and efficiency are shown in Figure 20. The proposed Jaya algorithm is compared to standard MPPT algorithms in the literature, such as P&O-INCO (Benyahia et al. 2014), fuzzy-PSO (Mallick and Mukherjee 2020), GWO-PID (Correa et al. 2004, 2004), ANFIS (Luta and Raji 2019), and SSA (Yang et al. 2017), shown in Table 4.

Conclusions

The Jaya algorithm-based MPPT controller of PEMFC was detailed in this paper in the context of enhancing output power and efficiency under varying operating scenarios. When compared to some contemporary MPPT approaches, the proposed technique has a greater degree of flexibility. In Jaya-based MPPT, the oscillation was observed to be minimal at steady-state compared to P&O and PSO, as Jaya algorithm preserves global peak solution once the optimal point is achieved until there is a change in operating conditions. The results indicated that the proposed approach is useful for tracking the optimized power of fuel cells accurately and timely manner. The performance of Jaya-based MPPT was tested and evaluated using five different instances of operating conditions. Jaya algorithm's output was compared to PSO and P&O approaches. In the first case, under normal operating scenario, temperature, MWC, hydrogen gas pressure, and oxygen gas pressure were $T = 300K$, $\lambda_m = 3, Ph_2 = 0.7$ atm, and $Po_2 = 0.8atm$, respectively, for which the maximum possible power of FC and related tracking time was $1189.7W$ and $0.12s$, respectively. The maximum power ratings obtained for PSO, P&O, and without MPPT were accordingly $1125.2W, 1113.42W$, and $980W$. When compared to PSO, P&O, and without MPPT, the Jaya approach improved maximum power by a percentage of $5.4\%, 6.4\%,$ and 17.62%, respectively. Jaya, PSO, P&O, and without MPPT tracking algorithms relative tracking efficiency was observed to be $99.14\%, 93.76\%, 92.78\%,$ and 81.6%, respectively. This work can be further extended by reducing the number of sensors to decrease system costs. Furthermore, the speed of the tracking time can be +further improved by amalgamating two or more heuristic approaches which can optimally reduce the search space.

Disclosure statement

No potential conflict of interest was reported by the author(s).

Funding

This work was supported by the Science and Engineering Research Board [EEQ/2016/000814].

ORCID

Ramesh Gugulothu http://orcid.org/0000-0003-1808-0718
Bhookya Nagu http://orcid.org/0000-0003-4728-455X
Deepak Pullaguram http://orcid.org/0000-0003-3401-5123

Nomenclature

D	Set of duty cycle	DC	Direct current
d	Duty ratio	ΔG	Gibbs free energy in (J/mol)
d_i^k	Actual value	ΔS	Entropy change of value
d_i^{k+1}	Upgraded value	CO_2	oxygen concentration in (mol cm^{-3})
d_{best}	Best function	E_{Nerst}	Reversible open-circuit output voltage

(*Continued*)

D	Set of duty cycle	DC	Direct current
d	Duty ratio	ΔG	Gibbs free energy in (J/mol)
d_i^k	Actual value	ΔS	Entropy change of value
d_i^{k+1}	Upgraded value	CO_2	oxygen concentration in (mol cm^{-3})
d_{best}	Best function	E_{Nerst}	Reversible open-circuit output voltage
d_{worst}	Worst function	i_L	Limiting current
e^-	Number of electrons	i_{FC}	Fuel cell current
H_2	Hydrogen gas	$r_1 and r_2$	Randomnumbers
H_2O	Water content	R_C	Lead contact resistance
N_{FC}	Number of fuel cells	R_M	Resistance of the fuel cell
O_2	Oxygen	r_m	Electrolyte membrane resistance Ω.cm
P_{FC}	Fuel cell output power	t_m	Thickness of the electrolyte membrane (0.0178cm)
Ph_2	Hydrogen gas partial pressure	T_o	Reference temperature (298K)
Ph_{2max}	Maximumsafepressureofthecylinder	V_{act}	Activation drop
Ph_{2min}	Minimumhydrogengasofthecylinder	V_{cell}	Single cell voltage
Po_2	Oxygengaspartialpressure	V_{con}	Concentration loss
V_{ohmic}	Ohmic loss	MPP	Maximum power point
V_{FC}	Fuel cell output voltage	MPPT	Maximum power point tracking
A	Activation area of the FC($232cm^2$)	MWC	Membrane water content (λm)
ALO	Ant- lion optimizer	n	Number of electrons contained in the reaction
ANFIS	Artificial neuro fuzzy inference system	P&O	Perturb and observe
ANN	Artificial neural network	PEMFC	Proton exchange membrane
BESS	Battery energy storage system	PID	Proportional integral derivative
CSO	Chicken swarm optimization	PSO	Particle swarm optimization
DE	Differential evolution	R	Universal constant of gas (8.314/K.mol)
ESSs	Energy storage systems	RES	Renewable energy sources
EVs	Electrical vehicles	SCA	Sine cosine algorithm
F	Faraday constant (96487C)	SSA	Slap swarm algorithm
FCs	Fuel cells	T	Temperature (343K)
FSS	Fixed step size	VSS	Variable step size
GWO	Grey wolf optimizer	WCA	Water cycle algorithm
INCO	Incremental conductance		
INRE	Incremental Resistance		

References

Agrawal, N., S. Samanta, and S. Ghosh, "Optimal state feedback-integral control of fuel-cell integrated boost converter," in IEEE Transactions on Circuits and Systems II: Express Briefs, 69(3), pp. 1382–1386. doi:10.1109/TCSII.2021.3117716, 2021.

Ahmadi, S., S. Abdi, and M. Kakavand. 2017a 07. Maximum power point tracking of a proton exchange membrane fuel cell system using pso-pid controller. *International Journal of Hydrogen Energy* 42 (32):20430–43. doi:10.1016/j.ijhydene.2017.06.208.

Ahmadi, S., S. Abdi, and M. Kakavand. 2017b. Maximum power point tracking of a proton exchange membrane fuel cell system using pso-pid controller. *International Journal of Hydrogen Energy* 42 (32):20 430–20 443.

Akbary, P., M. Ghiasi, M. R. R. Pourkheranjani, H. Alipour, and N. Ghadimi. 2019. Extracting appropriate nodal marginal prices for all types of committed reserve. *computational Economics* 53:1–26. doi:10.1007/s10614-017-9716-2.

Aly, M., and H. Rezk. 2020. A differential evolution-based optimized fuzzy logic mppt method for enhancing the maximum power extraction of proton exchange membrane fuel cells. *IEEE Access* 8:172 219–172 232. doi:10.1109/ACCESS.2020.3025222.

Ao, Y., S. Laghrouche, D. Depernet, and K. Chen. 2021. Proton exchange membrane fuel cell prognosis based on frequency-domain kalman filter. *IEEE Transactions on Transportation Electrification* 7 (4):2332–43. doi:10.1109/TTE.2021.3077506.

Benchouia, N. E., A. Derghal, B. Mahmah, B. Madi, L. Khochemane, and E. Hadjadj Aoul. 2015. An adaptive fuzzy logic controller (aflc) for pemfc fuel cell. *International Journal of Hydrogen Energy* 40 (39):13 806–13 819. doi:10.1016/j.ijhydene.2015.05.189.

Benyahia, N., H. Denoun, A. Badji, M. Zaouia, T. Rekioua, N. Benamrouche, and D. Rekioua. 2014. Mppt controller for an interleaved boost dc–dc converter used in fuel cell electric vehicles. *International Journal of Hydrogen Energy* 39 (27):15 196–15 205. doi:10.1016/j.ijhydene.2014.03.185.

Bhukya, L., and S. Nandiraju. 2020. A novel photovoltaic maximum power point tracking technique based on grasshopper optimized fuzzy logic approach. *International Journal of Hydrogen Energy* 45 (16):9416–27. doi:10.1016/j.ijhydene.2020.01.219.

Bizon, N. 2010. On tracking robustness in adaptive extremum seeking control of the fuel cell power plants. *Applied Energy* 87 (10):3115–30. doi:10.1016/j.apenergy.2010.04.007.

Bizon, N. 2017. Energy optimization of fuel cell system by using global extremum seeking algorithm. *Applied Energy* 206:458–74. doi:10.1016/j.apenergy.2017.08.097.

Bizon, N., M. Radut, and M. Oproescu. 2015. Energy control strategies for the fuel cell hybrid power source under unknown load profile. *Energy* 86:31–41. doi:10.1016/j.energy.2015.03.118.

Cai, W., R. Mohammaditab, G. Fathi, K. Wakil, A. G. Ebadi, and N. Ghadimi. 2019. Optimal bidding and offering strategies of compressed air energy storage: A hybrid robust-stochastic approach. *Renewable Energy* 143:1–8. doi:10.1016/j.renene.2019.05.008.

Caisheng Wang, M. H. N., S. R. Shaw, and S. R. Shaw. 2005. Dynamic models and model validation for pem fuel cells using electrical circuits. *IEEE Transactions on Energy Conversion* 20 (2):442–51. doi:10.1109/TEC.2004.842357.

Cha, S. W., R. O'Hayre, Y.-I. Park, and F. Prinz. 2006. Electrochemical impedance investigation of flooding in micro-flow channels for proton exchange membrane fuel cells. *Journal of Power Sources* 161 (1):138–42. doi:10.1016/j.jpowsour.2006.04.123.

Chen, P.-Y., K.-N. Yu, H.-T. Yau, J.-T. Li, and C.-K. Liao. 2017. A novel variable step size fractional order incremental conductance algorithm to maximize power tracking of fuel cells. *Applied Mathematical Modelling* 45:1067–75. doi:10.1016/j.apm.2017.01.026.

Correa, J. M., F. A. Farret, L. N. Canha, and M. G. Simoes. 2004. An electrochemical-based fuel-cell model suitable for electrical engineering automation approach. *IEEE Transactions on Industrial Electronics* 51 (5):1103–12. doi:10.1109/TIE.2004.834972.

Dargahi, M., M. Rezanejad, J. Rouhi, and M. Shakeri, "Maximum power point tracking for fuel cell in fuel cell/battery hybrid systems," in 2008 IEEE International Multitopic Conference, Karachi, Pakistan, 2008, pp. 33–37.

Derbeli, M., O. Barambones, and L. Sbita. 2018. A robust maximum power point tracking control method for a pem fuel cell power system. *Applied Sciences* 8 (12):2449. doi:10.3390/app8122449.

Derbeli, M., O. Barambones, M. Y. Silaa, and C. Napole. 2020. Real-time implementation of a new mppt control method or a dc-dc boost converter used in a pem fuel cell power system. *Actuators* 9 (4):105. doi:10.3390/act9040105.

Egiziano, L., A. Giustiniani, G. Petrone, G. Spagnuolo, and M. Vitelli, "Optimization of perturb and observe control of grid connected pem fuel cells," in 2009 International Conference on Clean Electrical Power, Capri, Italy., 2009, pp. 775–81.

Fathabadi, H. 2016. Novel high-efficient unified maximum power point tracking controller for hybrid fuel cell/wind systems. *Applied Energy* 183:1498–510. doi:10.1016/j.apenergy.2016.09.114.

Fathy, A., M. A. Abdelkareem, A. Olabi, and H. Rezk. 2021. A novel strategy based on salp swarm algorithm for extracting the maximum power of proton exchange membrane fuel cell. *International Journal of Hydrogen Energy*. developments of Hydrogen Fuel Cell Technologies. 46 (8):6087–99. doi:10.1016/j.ijhydene.2020.02.165.

Harrabi, N., M. Souissi, A. Aitouche, and M. Chaabane. 2018. Modeling and control of photovoltaic and fuel cell based alternative power systems. *International Journal of Hydrogen Energy*. alternative Energies for Sustainability. 43 (25):11 442–11 451. doi:10.1016/j.ijhydene.2018.03.012.

Harrag, A., and H. Bahri. 2017. Novel neural network ic-based variable step size fuel cell mppt controller: Performance, efficiency and lifetime improvement. *International Journal of Hydrogen Energy* 42 (5):3549–63. doi:10.1016/j.ijhydene.2016.12.079.

Harrag, A., and S. Messalti. 2018. How fuzzy logic can improve pem fuel cell mppt performances? *International Journal of Hydrogen Energy* 43 (1):537–50. doi:10.1016/j.ijhydene.2017.04.093.

Huang, C., L. Wang, R. S. Yeung, Z. Zhang, H. S. Chung, and A. Bensoussan. 2018. A prediction model-guided jaya algorithm for the pv system maximum power point tracking. *IEEE Transactions on Sustainable Energy* 9 (1):45–55. doi:10.1109/TSTE.2017.2714705.

Islam, M. M., S. A. Siat, I. Ahmad, M. Liaquat, and S. A. Khan. 2021. Adaptive nonlinear control of unified model of fuel cell, battery, ultracapacitor and induction motor based hybrid electric vehicles. *IEEE Access* 9:57 486–57 509. doi:10.1109/ACCESS.2021.3072478.

Jyotheeswara Reddy, K., and N. Sudhakar. 2018. High voltage gain interleaved boost converter with neural network based mppt controller for fuel cell based electric vehicle applications. *IEEE Access* 6:3899–908. doi:10.1109/ACCESS.2017.2785832.

Karami, N., L. E. Khoury, G. Khoury, and N. Moubayed, "Comparative study between p and o and incremental conductance for fuel cell mppt," in Second International Conference on Renewable Energies for Developing Countries (REDEC 2014), Beirut, Beyrouth, Lebanon., Nov 2014, pp. 17–22.

Khan, M. S., I. Ahmad, and F. Z. Ul Abideen. 2019. Output voltage regulation of fc-uc based hybrid electric vehicle using integral backstepping control. *IEEE Access* 7:65 693–65 702. doi:10.1109/ACCESS.2019.2912511.

Kim, N.-G., B. Han, S.-W. Jo, and M. Kim. 2021. High-voltage-gain soft-switching converter employing bidirectional switch for fuel-cell vehicles. *IEEE Transactions on Vehicular Technology* 70 (9):8731–43. doi:10.1109/TVT.2021.3100008.

Kirubakaran, A., S. Jain, and R. Nema. 2009. A review on fuel cell technologies and power electronic interface. *Renewable and Sustainable Energy Reviews* 13 (9):2430–40. doi:10.1016/j.rser.2009.04.004.

Kuan, Y.-D., J.-Y. Chang, and H.-T. Ku. 2017. Proton exchange membrane fuel cell purge and fan control using a microcontroller. *International Journal of Green Energy* 14 (1):86–91. doi:10.1080/15435075.2016.1206011.

Kumar, S., and B. Shaw. 2019. *"Design of off–grid fuel cell by implementing alo optimized pid-based mppt controller, in Soft Computing in Data Analytics*. In Eds. J. Nayak, A. Abraham, B. M. Krishna, G. T. C. Sekhar, and A. K. Das, 83–93. Singapore: Springer Singapore.

Larminie, J., A. Dicks, and M. S. McDonald. 2003. Fuel cell systems explained. *J. Wiley Chichester, UK* 2:67–118.

Li, Q., W. Chen, Z. Liu, A. Guo, and S. Liu. 2013. Control of proton exchange membrane fuel cell system breathing based on maximum net power control strategy. *Journal of Power Sources* 241:212–18. doi:10.1016/j.jpowsour.2013.04.067.

Liu, J., C. Chen, Z. Liu, K. Jermsittiparsert, and N. Ghadimi. 2020. An igdt-based risk-involved optimal bidding strategy for hydrogen storage-based intelligent parking lot of electric vehicles. *Journal of Energy Storage* 27:101057. doi:10.1016/j.est.2019.101057.

Liu, J., T. Zhao, and Y. Chen. 2017. Maximum power point tracking with fractional order high pass filter for proton exchange membrane fuel cell. *IEEE/CAA Journal of Automatica Sinica* 4 (1):70–79. doi:10.1109/JAS.2017.7510328.

Luta, D. N., and A. K. Raji. 2019. Fuzzy rule-based and particle swarm optimisation mppt techniques for a fuel cell stack. *Energies* 12 (5):936. doi:10.3390/en12050936.

Mallick, N., and V. Mukherjee. 2020. Maximum power point tracking supported proton exchange membrane fuel cell based intelligent dynamic voltage restorer. *International Journal of Hydrogen Energy* 45 (53):29 271–29 287. doi:10.1016/j.ijhydene.2020.07.185.

Mohamed, P., K. Chandrakala, and S. Subramani, "Comparative study of maximum power point tracking techniques for fuel cell powered electric vehicle," IOP Conference Series: Materials Science and Engineering, United Kingdom, vol. 577, p. 012031, 12 2019.

Mungporn, P., P. Thounthong, B. Yodwong, C. Ekkaravarodome, A. Bilsalam, S. Pierfederici, D. Guilbert, B. Nahid Mobarakeh, N. Bizon, Z. Shah, et al. 2020. Modeling and control of multiphase interleaved fuel-cell boost converter based on Hamiltonian control theory for transportation applications. *IEEE Transactions on Transportation Electrification* 6 (2):519–29. doi:10.1109/TTE.2020.2980193.

Nasiri Avanaki I, S. M. 2016. A new maximum power point tracking method for pem fuel cells based on water cycle algorithm. *J Renew Energy Environ* 3(1):35–42. https://Www.Sid.Ir/En/Journal/Viewpaper.Aspx?Id=491386 .

Nasiri Avanaki, I., and S. Mohammad. 2016. A new maximum power point tracking method for pem fuel cells based on water cycle algorithm. *Journal of Renewable Energy and Environment* 3 (1):35–42.

Pasricha, S., and S. R. Shaw. 2006. A dynamic pem fuel cell model. *IEEE Transactions on Energy Conversion* 21 (2):484–90. doi:10.1109/TEC.2005.860402.

Priyadarshi, N., F. Azam, S. Solanki, A. Sharma, A. K. Bhoi, and D. Almakhles. 01, 2021. A bio-inspired chicken swarm optimization-based fuel cell system for electric vehicle applications. 297–308. doi:10.1007/978-981-15-5495-7_16.

Raj A, L. P., "An anfis based mppt controller for fuel cell powered induction motor drive," In Proceedings of the 2018 International Conference on Smart Grid and Clean Energy Technologies (ICSGCE) Kuala Lumpur, Malaysia, p. 201–05, 2018.

Rana, K., V. Kumar, N. Sehgal, and S. George. 2019. A novel dpdi feedback based control scheme using gwo tuned pid controller for efficient mppt of pem fuel cell. *ISA Transactions* 93:312–24. doi:10.1016/j.isatra.2019.02.038.

Reddy, K., and D. S. Natarajan. 2019a. Anfis-mppt control algorithm for a pemfc system used in electric vehicle applications. *International Journal of Hydrogen Energy* 44 (29):04. doi:10.1016/j.ijhydene.2019.04.054.

Reddy, K., and D. S. Natarajan. 2019b. Anfis-mppt control algorithm for a pemfc system used in electric vehicle applications. *International Journal of Hydrogen Energy* 44 (29):04.

Rezk, H., and A. Fathy. 2020. Performance improvement of pem fuel cell using variable step-size incremental resistance mppt technique. *Sustainability* 12 (14):5601. doi:10.3390/su12145601.

Samal, S., R. Makireddi, and P. K. Barik. 2018. Modeling and simulation of interleaved boost converter with mppt for fuel cell application. 03:1–5. doi:10.1109/ICSESP.2018.8376704.

Sarvi M, B. M., "45th international universities power engineering conference," UPEC 2010 : 45th International Universities Power Engineering Conference, Cardiff, United Kingdom. IEE E2010, pp. 2010.

Shashikant, and B. Shaw. 2019. Comparison of sca-optimized pid and p&o-based mppt for an off-grid fuel cell system. In *Soft computing in data analytics*, ed. J. Nayak, A. Abraham, B. M. Krishna, G. T. C. Sekhar, and A. K. Das, 51–58. Singapore: Springer Singapore.

Shen, D., -C.-C. Lim, and P. Shi. 2020. Robust fuzzy model predictive control for energy management systems in fuel cell vehicles. *Control Engineering Practice* 98:104364. doi:10.1016/j.conengprac.2020.104364.

Sorlei, I.-S., N. Bizon, P. Thounthong, M. Varlam, E. Carcadea, M. Culcer, M. Iliescu, and M. Raceanu. 2021. Fuel cell electric vehicles—a brief review of current topologies and energy management strategies. *Energies* 14 (1):252. doi:10.3390/en14010252.

Thounthong, P., and B. Davat. 04, 2010. Study of a multiphase interleaved step-up converter for fuel cell high power applications. *Energy Conversion and Management – Energ Conv Manage*. 51:826–32. doi:10.1016/j.enconman.2009.11.018.

Torreglosa, J. P., P. Garc´ıa, L. M. Fern´andez, and F. Jurado. 2014. Predictive control for the energy management of a fuel-cell–battery–supercapacitor tramway. *IEEE Transactions on Industrial Informatics* 10 (1):276–85. doi:10.1109/TII.2013.2245140.

Venkata Rao, R. 2016. Jaya: A simple and new optimization algorithm for solving constrained and unconstrained optimization problems. *International Journal of Industrial Engineering Computations* 7:19–34, 01. doi:10.5267/j.ijiec.2015.8.004.

Wang, M. H., M.-L. Huang, W.-J. Jiang, and K.-J. Liou. 2016. Maximum power point tracking control method for proton exchange membrane fuel cell. *IET Renewable Power Generation* 10 (7):908–15. doi:10.1049/iet-rpg.2015.0205.

Wang, C., and M. H. Nehrir. 2007. Load transient mitigation for stand-alone fuel cell power generation systems. *IEEE Transactions on Energy Conversion* 22 (4):864–72. doi:10.1109/TEC.2006.881081.

Yang, Z., M. Ghadamyari, H. Khorramdel, S. M. Seyed Alizadeh, S. Pirouzi, M. Milani, F. Banihashemi, and N. Ghadimi. 2021. Robust multi-objective optimal design of islanded hybrid system with renewable and diesel sources/stationary and mobile energy storage systems. *Renewable and Sustainable Energy Reviews* 148:111295. doi:10.1016/j.rser.2021.111295.

Yang, X., L. Shu, J. Chen, A. Ferrag Mohamed, J. Wu, E. Nurellari, and K. Huang. 2017. "Ieee/caa journal of automatica sinicae," IEEE/CAA, Beijing, China.

Ye, H., G. Jin, W. Fei, and N. Ghadimi. 2020. High step-up interleaved dc/dc converter with high efficiency. *Energy Sources, Part A: Recovery, Utilization, and Environmental Effects*:1–20.

Zhang, M., T. Yan, and J. Gu. 2014. Maximum power point tracking control of direct methanol fuel cells. *Journal of Power Sources* 247:1005–10. doi:10.1016/j.jpowsour.2013.06.152.